NUMERICAL MODELLING, SIMULATION AND VALIDATION OF THE SPS AND PS SYSTEMS UNDER 6 KG TNT BLAST SHOCK WAVE

Marek ŚWIERCZEWSKI*, Marian KLASZTORNY*, Paweł DZIEWULSKI*, Paweł GOTOWICKI*

*Department of Mechanics and Applied Computer Science, Faculty of Mechanical Engineering, Military University of Technology, ul. Gen. S. Kaliskiego 2, 00-908 Warszawa, Poland

mswierczewski@wat.edu.pl, mklasztorny@wat.edu.pl, pdziewulski@wat.edu.pl, pgotowicki@wat.edu.pl

Abstract: The paper develops a new methodology of FE modelling and simulation of the SPS and SP systems under 6 kg TNT blast shock wave. SPS code refers to the range stand – protected plate – protective shield ALF system, while PS code refers to the range stand – protected plate system. The multiple – use portable range stand for testing protective shields against blast loadings was developed under Research and Development Project No. O 0062 R00 06. System SPS uses high strength M20 erection bolts to connect the protective shield to the protected plate. In reference to the SPS system, validation explosion test was performed. It has pointed out that the developed methodology of numerical modelling and simulation of SPS and PS systems, using CATIA , HyperMesh, LS-Dyna, and LS-PrePost software, is correct and the ALF protective shield panels have increased blast resistance and high energy – absorption capability.

Key words: Military Vehicle, Passive Shield, Range Stand, Protected Plate, Blast Shock Wave, Numerical Modelling, Simulation, Range Tests, Validation

1. INTRODUCTION

Within the framework of Research and Development Project No. O 0062 R00 06 (Klasztorny, 2010a) the authors' team has designed the ALF energy-absorbing shield and the portable range stand for testing protective shields against shock wave loading induced by blast of a spherical charge up to 6 kg of TNT. The ALF shield is purposed for protection of crew-occupants of military vehicles against blast and fragmentation of AT mines and IED devices for selected protection levels. Papers (Klasztorny, 2010b, c) present numerical modeling, simulations and experimental validation of the SPS and PS systems loaded by 2 kg TNT blast shock wave. The SPS code is referred to as the range stand – protected plate – ALF shield system while the PS code denotes the range stand – protected plate system. In the case of 2 kg of TNT charge the ALF square segment was glued to the protected plate. At larger HE charges erection bolts must be applied.

The paper develops a new methodology of FE modelling and simulation of SPS and SP systems under 6 kg TNT blast shock wave. In SPS system four bolt connections were used to join the energy-absorbing shield to the protected plate. In reference to the SPS system the validation range test is presented. The parameter modification of laminas of the hybrid laminates has been examined in order to eliminate non-physic erosion of the composite finite elements. The physic damping has been limited to the protected plate in order to achieve better convergence of the explicit algorithm (Hallquist, 2009). The literature review has been presented in (Klasztorny, 2010b).

2. DESCRIPTION OF THE SPS SYSTEM

The ALF energy-absorbing shield is purposed for protection of crew-occupants of logistic vehicles (LV) and light armoured vehicles (LAV) against blast and fragmentation of AT mines and IED devices under the vehicle body shell.

The tactical – technological assumptions related to the ALF shield, formulated according to standards (AEP, STANAG), are collected below:

- the shield is purposed to modernize serviced LV and LAV vehicles (without any modifications of the vehicle body bottom) and to design new types of military vehicles;
- the shield has modular structure;
- structural layers of the shield panels have plate shape and are joined together with glue;
- the shield is non-flammable, resistant to atmospherical and chemical factors;
- the shield thickness does not exceed 76 mm;
- the maximum shield mass per unit area equals 50 kg/m^2;
- thickness of the protected steel plate modelling the vehicle body bottom plate equals 5÷8 mm;
- high energy-absorbing materials are applied as components of the shield;
- the maximum overall dimensions of the shield panels amount to 700×700 mm;
- the shield panels are exchangeable directly on the vehicle using bolt connections;
- a simple manufacturing, assembly and disassembly technology in reference to the shield panels must be developed;
- the shield is characterised by long durability and low material – production costs;
- the layered structure of the shield must be developed in such a way to achieve the highest protection level of crew-occupants of LV and LAV vehicles against blast and fragmentation of AT mines and IED devices under the vehicle body shell.

The ALF shield has sandwich structure with cover shells made of hybrid laminate in the form of special combination of uniform

laminates. The latter are manufactured using the following components:

- incombustible VE 11-M vinylester resin matrix produced by Organika-Sarzyna Chemical Plant, Poland;
- Style 430 / Tenax HTA40 6K plain weave carbon fabric, 300 g/m^2 substance, 400/400 tex warp/weft, 3,7/3,7 strand/cm, produced by C. Cramer GmbH & Co. KG Division ECC;
- Style 328 / Kevlar 49 T 968 / T 968 TG aramid plain weave fabric, 230 g/m^2 substance, 158/158 tex warp/weft, 7/7 strand/cm, produced by C. Cramer GmbH & Co. KG Division ECC;
- S SWR 800 glass plain weave fabric, 800 g/m^2 substance, produced by Hongming Composites CO., Ltd.

Useful properties of VE 11-M vinylester resin matrix corresponding to the adopted assumptions, are as follows:

- neutral resin with good moulding properties;
- good saturatability of fibres;
- high elasticity;
- incombustibility;
- high chemical and thermal resistance;
- high relative tensile strength;
- high relative stiffness;
- high resistance to atmospheric factors and service pollutants,
- long durability;
- anti-vibrating resistance.

The following uniform laminates have been designed and used in hybrid laminates (Klasztorny, 2010a):

- the vinylester–carbon regular cross–ply laminate (C/VE); laminas composed of VE 11-M resin and Style 430 carbon fabric with fibre volume/mass fraction f_V=54,4%, f_m=68,0%,
- the vinylester–aramid regular cross–ply laminate (A/VE); laminas composed of VE 11-M resin and Style 328 aramid fabric with fibre volume/mass fraction f_V=48,3%, f_m=57,5%,
- the vinylester–glass regular cross–ply laminate (S/VE); laminas composed of VE 11-M resin and SWR800 S glass fabric with fibre volume/mass fraction f_V=53,5%, f_m=73,7%.

Hybrid laminate plates, manufactured using the vacuum technology, are 24-ply composites with the specified sequence of GFRP, CFRP and KFRP laminates. Based on the preliminary ballistic tests, performed on selected configurations of uniform laminates (Klasztorny, 2010a), the final symmetric SCACS hybrid laminate has been designed to apply it in ALF protective shields, with the ply sequence of:

$$\{[(0/90)_{SF}]_2\ [(0/90)_{CF}]_4\ [(0/90)_{AF}]_6\ \}_S \qquad (1)$$

where: SF – SWR800 S glass fabric, CF – Style 430 carbon fabric, AF – Style 328 aramid fabric. Thicknesses of uniform laminate components respectively are equal to 1,3; 1,3; 3,8; 1,3; 1,3 mm (9 mm in total).

The following properties of hybrid laminate components have been utilized:

- high tensile strength of Carbon 6K (Style 430, ECC) fibres;
- high elasticity of Kevlar 49 T 968 aramid fibres;
- high impact resistance SWR800 S glass fibres;
- high elasticity of VE 11-M vinylester resin;
- maximum ballistic resistance of the SCACS stacking configuration;
- fire resistance, chemical resistance and resistance to atmospheric factors of VE 11-M vinylester resin.

Semi-finished products of SCACS hybrid laminates have been manufactured using the vacuum technology by ROMA Ltd. Grabowiec, Poland. The vacuum pressing technology developed by ROMA Ltd. is described below:

- stacking of reinforcement and resin layers (50% gravimetrically);
- pressing in the closed mould with Vacuum connected;
- air removing and pressure on the mould through partial vacuum -0.03/-0.04 MPa;
- the composite curing;
- seasoning over 24 hours;
- removing the composite from the mould;
- mechanical working (cutting off technological allowances);
- after stove at 70°C over 3 hours.

The parameters for curing and after stove of VE 11-M resin matrix were compatible with Material Card published by the producer (Organika-Sarzyna Chemical Plant, Sarzyna, Poland).

Taking into consideration the tactical – technological assumptions for the layered shield and the literature review results, Authors' team has designed the shield having the stacking structure set up in Tab. 1 and illustrated in Figs. 1 and 2. The shield has bestowed the ALF code (Aluminium – Laminate – Foam protective panel). The mass per unit area equals 50 kg/m^2, and the thickness equals 76 mm including glue joining layers.

Tab. 1. The stacking structure of the ALF shield for LV/LAV crew-occupants protection from blast and fragmentation of AT mines/ IED devices (Klasztorny, 2010a)

Layer No.	Specificatio (from the impact side)	thickness [mm]
1	PA11 (EN AW-5754) aluminium	2
2	Soudaseal 2K glue	2
3	SCACS hybrid laminate	9
4	Soudaseal 2K glue	2
5	ALPORAS aluminium foam	50
6	Soudaseal 2K glue	2
7	SCACS hybrid laminate	9
	Total	**76**

The shield components are joined with Soudaseal 2K chemoset glue exhibiting good adherence to metals and composites. It is characterized by high hardness (55 in Shore A scale), good mechanical properties, good resistance to atmospheric factors and limited chemical resistance. This glue is designed to make elastic connections exposed to heavy vibrations which are well damped. The thermal resistance of the glue is close to the VE 11-M resin matrix.

The layer No. 1 (aluminium plate) is the head layer carrying the thermal impact and protecting shield–plate assembling with erection bolts. The layers No. 2, 7 (hybrid laminates) are energy-absorbing resistant layers. The blast impact energy is absorbed utilizing the following progressive failure mechanisms: shear, delamination, bending. The alyer No. 5 (aluminium foam) is the central high energy-absorbing resistant layer. The blast impact energy is absorbed utilizing the following progressive failure mechanisms: compression, disruption, shear. Aluminium foam is the core of the sandwich panel, enabling carrying high bending moments and shear forces. Three glue layers enlarge flexibility of the shield, induce multiple reflected waves when the blast

impact wave crosses the shield. In this way, the protected plate is impacted by the wave of weaker impulse pressure.

The LV/LAV vehicle protective shield is divided into panels shaped and dimensioned according to the shape and dimensions of the vehicle body shell bottom. In the failure case the panels are exchanged. The maximum overall dimensions of the panels are 500×500 mm. The panels are connected to the vehicle bottom plate with erection bolts having increased strength and protection against unbolting. There are used M16 bolts with heads welded point wisely on vehicle bottom plate, from the vehicle body inside and using self-blocking shaped nuts (Figs. 1 and 2).

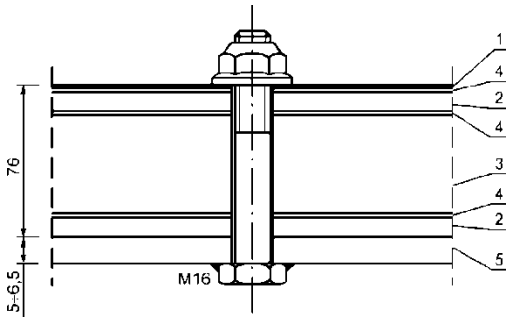

Fig.1. The bolt connection of the ALF shield to the protected plate: 1 – aluminium plate, 2 – hybrid laminate, 3 – aluminium foam, 4 – glue, 5 – protected plate

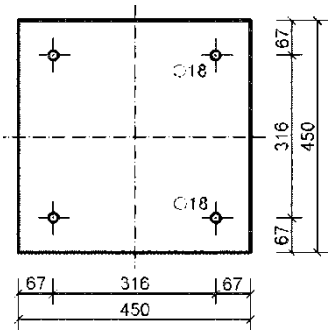

Fig. 2. The top view on the ALF square panel used in range tests (the holes for the erected bolts are depicted)

A multiple-use portable range stand for blast tests up to 6 kg of TNT, named with code BTPS, is shown in Figs. 3 and 4. The stand has the following specification:

- The BTPS stand is composed of three closed, horizontal, steel frames, respectively graded and connected together with six high strength 10.9 M20 erection bolts. Normal washers make possible unbolting after each blast test in order to exchange the tested subsystem (the protective plate or the shield–plate subsystem). The nuts are protected with cups. The holes for bolts are with passage with head blocking in the horizontal recesses in the bottom frame. The holes have 2 mm clearance.
- Each frame has mass ~100 kg. The frames are equipped with carrying handles for four persons (25 kg per person).
- The protected plate, without or with the protective panel, has dimensions 650×650×*h* mm (*h*=5÷6,5 mm) and is put in the 7 mm thick horizontal recess in the central frame. The plate is initially put eccentrically in the recess zone and next shifted into the recess and positioned centrally.
- The protected plate is fixed between two frames with possible travelling and friction. This solution ensures selection of the energy absorbed by the protected plate or the shield–plate subsystem. For the 5 mm thick protected plate the clearance between the protected plate supported strips and the top frame amounts to 2 mm. The friction is repeatable in subsequent tests.
- The width of the supported plate strip equals 90 mm on the whole perimeter of the plate. It protects the plates against line feed from the perimeter gap at HE charges up to 6 kg of TNT.
- The energy-absorbing panel has the overall dimensions 450×450×65 mm. The perimeter clearance between the shield and the top frame equals 10 mm to make the assembly easy and to unblock the panel failure during the blast test.
- There are incorporated plain scarfs on the internal perimeter of the top frame at angle of 26° that protect the tested subsystem from the wave reflected from the top frame.
- The stand frames are dimensioned under condition of elastic strains and small deflections under blast shock waves induced by HE charges up to 6 kg of TNT. The frames are made of 790×650×60 mm St3S steel flats.
- Meshes of the frames have horizontal clearances in order to make the assembly easier.
- The stand rests on the 900×850×20 mm steel plate having the central square hole of dimensions 450×450 mm. Under the plate the 450×450×300 mm central free space in the subsoil is done. The subsoil has increased stiffness.
- The HE charge is hanged centrally over the stand 400 mm from the top surface frame.

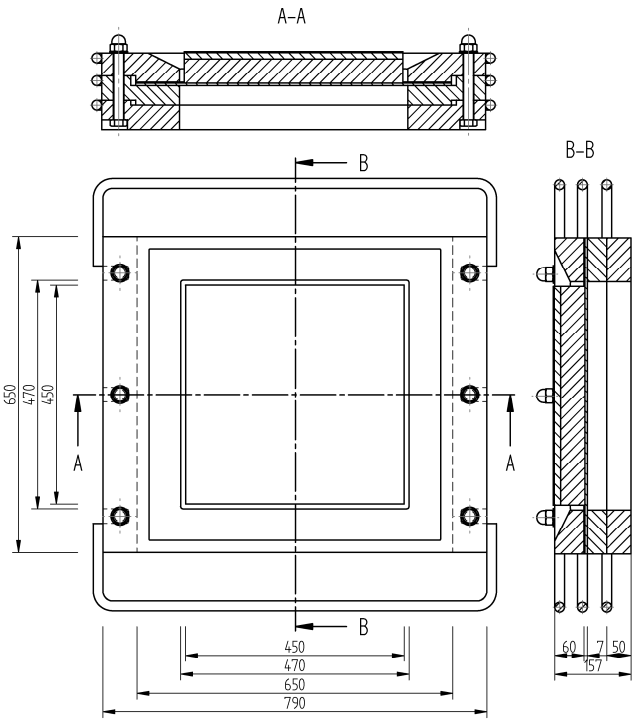

Fig. 3. The basic dimensions and main cross-sections of the BTPS range stand (Klasztorny, 2010a)

The three closed thick frames creating the BTPS stand body, respectively profiled and joined together, make possible performing blast tests up to 6 kg of TNT in such a way that:

- the stand body deforms elastically;
- the protected plate has freedom of movement and strains between the top and central frames;
- the protected plate may deform plastically and the protective

panel may by fully destroyed.

In the simulations and range tests, the 6 kg TNT spherical charge was applied, suspended centrally over the SPS system, distanced by 400 mm from the top frame surface. A detonator was placed centrally inside the sphere. The 5 mm thick protected plate was made of Armox 500T armoured steel.

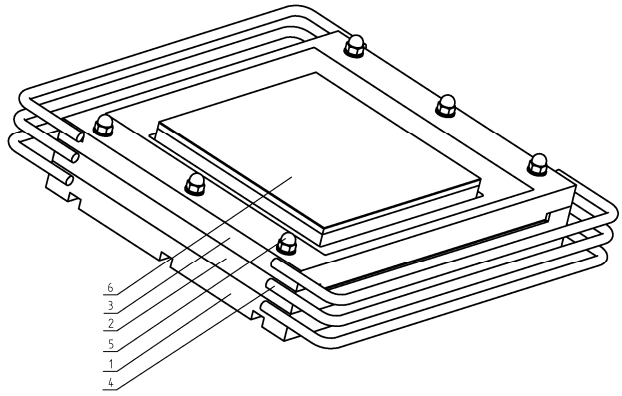

Fig. 4. The assemblied BTPS range stand: 1 – bottom frame, 2 – central frame, 3 – top frame, 4 – handle, 5 – bolt, 6 – protective panel (Klasztorny, 2010a)

3. NUMERICAL MODELLING OF THE PS AND SPS SYSTEMS

The FEM numerical modelling, simulation and postprocessing in reference to the PS and SPS systems under blast shock wave were developed using the following CAE systems: CATIA, HyperMesh, LS-Dyna, LS-PrePost.

The geometrical models of the PS and SPS systems were built using CATIA system. The FE meshing in particular subsystems was generated automatically using HyperMesh platform. LS-PrePost programme was used as a pre-processor to define the boundary conditions, finite elements, material properties, the solution type. Complete FE model was exported as a key file with LS-Dyna preferences. LS-Dyna programme was used as a solver and LS-PrePost programme was applied as the post-processor.

The 8-node 24 DOF brick finite elements were used, taking into account contact and friction phenomena. The FE model of the protected plate – range stand (PS) system has about 98000 DOFs, whereas the FE model of the protective shield – protected plate – range stand (SPS) system has about 282000 DOFs. The FE models are relatively dense and finite elements' dimensions satisfy the aspect ratio condition before and during the blast loading. For the composite layers 1–Gauss point integration (ELFORM 1) and hourglass control were applied. For the remaining structural components 8–Gauss point integration (ELFORM 2) was adopted. The horizontal dimensions of most FEs were 5×5 mm. Thicknesses of FE layers were assumed to satisfy the aspect ratio before and during dynamic process (Hallquist, 2009). Quantities and thicknesses of the FE layers in particular components of the modelled system are collected in Tab. 2.

Uniform laminates S (2 layers), C (4 layers) can be modelled as single equivalent layers since mechanical properties of these laminates were identified experimentally in macroscale (e.g. interlaminar shear strength) and the ply sequences are limited to $[0/90]_n$. The thicker A laminate was reflected by three layers; it means that each FE layer reflects 4 laminate layers. The reasons for such FE meshing given for S and C laminates are also valid for A laminate.

The aluminium foam layer is modelled as equivalent homogenized solid body. The 10 mm thick FE layers protect aspect ratio before and after foam compaction.

Tab. 2. Quantities and thicknesses of the FE layers in particular components of the SPS numerical model

Component of the PS/SPS system	Layers quantity	Layer thickness [mm]
aluminium sheet	1	2
glue	2	1
S laminate	1	1.3
C laminate	1	1.3
A laminate	3	1.27
aluminium foam	5	10
protected plate	3	1.67

The erection bolts in the range stand are designed to work in the elastic range, so they can be modelled approximately as bars with the equivalent square cross-section. The erection bolts in the ALF panels were modelled more accurately, i.e. with circular cross-sections taken into account. The stiffened subsoil was limited to the cubicoidal volume 2000×2000×1000 mm.

Because of bisymmetry of the PS and SPS systems, their numerical models were limited to respective quarters of the global systems. The boundary conditions in the planes of symmetry eliminate displacements perpendicular to these planes. The numerical models of the PS and SPS systems are shown in Figs. 5 and 6.

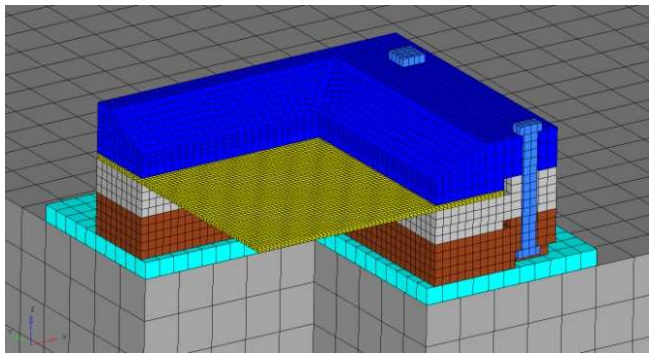

Fig. 5. Components of the PS system resting on the supporting plate and the subsoil (FE mesh of the system quarter)

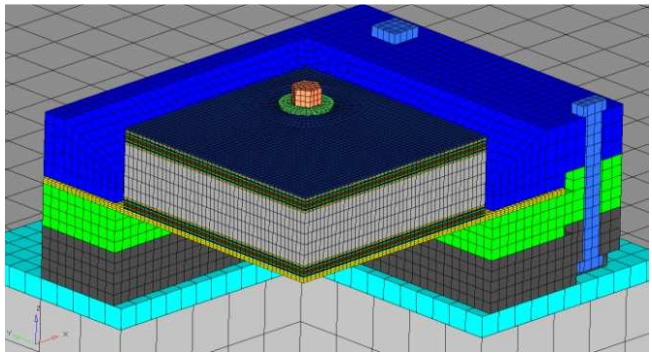

Fig. 6. Components of the SPS system resting on the supporting plate and the subsoil (FE mesh of the system quarter)

Material models for subsequent parts of the SPS system have been assumed from (Klasztorny, 2010a; Hallquist, 2009; Nillson, 2003; STANAG). In the materials' description original notation of input data assumed in FE code LS-Dyna as well as a system of units used in the numerical modelling and simulation (kg, mm, msec, K, GPa, kN) have been saved.

Armox 500T steel and PA11 aluminum
LS-Dyna material type 15: MAT_15
(MAT_JOHNSON_COOK)
Equation-of-state: EOS_GRUNEISEN

This is the Johnson–Cook strain and temperature sensitive plasticity material, used for problems where strain rates vary over a large range and adiabatic temperature increases due to plastic heating cause material softening. The model requires equation-of-state. Material data for Armox 500T steel and PA11 aluminium are collected in Tab. 3.

Tab. 3. Material constants for Armox 500T steel and PA11 aluminium

Parameter	Armox 500T	PA11
Mass density, RO	7.85e-6	2.815e-6
Shear modulus, G	79.6	28.6
Scale yield stress, VP	0	0
Flow stress: A B N C M	0.849 1.34 0.0923 0.00541 0.870	0.369 0.684 0.730 0.00830 1.70
Melt temperature, TM	1800	775
Room temperature, TR	293	293
Quasi-static threshold strain rate, EPSO	0.001	0.01
Specific heat , CP	450	875
Spall type , SPALL	2	2
Plastic strain iter. option, IT	1	1
Failure par.: D1 D2, D3, D4, D5	0.50 0	1.50 0
Intercept C	4570	5328
Slope coeff.: S1 S2, S3	1.49 0	1.338 0
Gruneisen gamma GAMAO	1.93	2.00
First order vol. correction A	0.50	0.48
Initial internal energy E0	0	0
Initial relative volume V0	1	1

Tab. 4. Material constants for components working in the elastic range

parameter	St3 steel	10.9 bolt steel	range subsoil
Mass density, RO	7.85e-6	7.85e-6	1.00e-6
Young's modulus, E	210	210	0.300
Poisson's ratio, PR	0.30	0.30	0.20
Yield stress, SIGY	0.33	0.90	2.5e-4
Tangent modulus, ETAN	1.00	1.00	1e-8
Plastic strain to failure, FAIL	0.50	0.50	1.00

Tab. 5. The average values of material constants for uniform composites S, C, A

Parameter	S	C	A
Mass density, RO	1.81e-6	1.45e-6	1.24e-6
Young's modulus in long. direction, EA	29	60	29
Young's modulus in transverse direction, EB	29	60	29
Young's modulus in through thickness direction, EC	9.8	7.2	3.9
Poisson's ratios: PRBA PRCA=PRCB	0.15 0.22	0.044 0.052	0.08 0.070
Shear moduli: GAB GBC=GCA	4.7 3.8	4.6 3.7	1.4 1.1
Material axes option: globally orthotropic, AOPT	2	2	2
Material axes change flag: no change, MACF	1	1	1
Layer in-plane rotational angle (degrees), BETA	0	0	0
Longitudinal tensile strength, SAT	0.439	0.624	0.579
Longitudinal compressive strength, SAC	0.335	0.580	0.0538
Transverse tensile strength, SBT	0.439	0.624	0.579
Transverse compressive strength, SBC	0.335	0.580	0.538
Trough thickness tensile strength, SCT	0.080	0.080	0.080
Crush strength, SFC	0.335	0.581	0.728
Fibre mode shear strength, SFS	0.056	0.046	0.031
Matrix mode shear strength in principal planes: SAB SBC=SCA	0.040 0.040	0.040 0.040	0.040 0.040
Scale factor for residual compressive strength, SFFC	0.10	0.10	0.10
Material model: fabric layer model, AMODEL	2	2	2
Coulomb friction angle for matrix and delamination failure (degrees), PHIC	14	14	14
Element eroding axial strain, E_LIMIT	0.035	0.035	0.035
Scale factor for delamination criterion, S_DELM	1	1	1
Limit compressive volume strain for element eroding, ECRSH	0.109	0.109	0.109
Limit tensile volume strain for element eroding, EEXPN	0.109	0. 109	0.109
Coefficients for strain rate	0	0	0

St3 steel, 10.9 bolt steel and hardened range subsoil
LS-Dyna material type: MAT_24
(MAT_PIECEWISE_LINEAR_PLASTICITY)

This is an elasto-plastic material with an arbitrary stress vs. strain curve and arbitrary strain rate dependency. St3 steel has been used for manufacturing the range stand and the bottom plate that stiffens the subsoil. The 10.9 steel is used to manufacture

M20 erection bolts. Material data are taken from (Klasztorny, 2010b). Input data for St3 steel, 10.9 bolt steel and hardened range subsoil are set up in Tab. 4. These components work in the elastic range at high margin safety; it explains why the static properties have been taken into account.

Plain weave fabric composites
LS-Dyna material type: MAT_161
(MAT_COMPOSITE_MSC)

This model is used to reflect the progressive failure criteria, including delamination, in composites consisting plain weave fabric layers. The failure criteria have been established by adopting the methodology developed by Hashin. The ply sequence type is $[(0/90)_{WF}]_n$, where subscript WF denotes woven fabric. In-plane principal directions are denoted as A and B, whereas out-of-plane principal direction is C. Material data, based on the standard experiments performed by Authors (average values), are set up in Tab. 5. Part of the material parameters were estimated from the rule of mixtures.

ALPORAS aluminium foam
LS-Dyna material type: MAT_26 (MAT_HONEYCOMB)

This material model is useful for honeycomb and foam materials. A nonlinear elasto-plastic behaviour is defined separately for all normal and shear stresses considered to be fully uncoupled. After homogenization, aluminium foam is modelled as an orthotropic material. The elastic moduli vary from the initial uncompacted values to the fully compacted values. The normal stress vs. volumetric strain load curve in the uniaxial compression test, in the form required by LS-Dyna code, is presented in Fig. 7. Material data are based on the Material Card and on the experiments executed by Authors:

- Mass density RO=0.23e-6;
- Young's modulus for fully compacted material E=70;
- Poisson's ratio for fully compacted material PR=0.30;
- Yield stress for fully compacted material SIGY=0.125;
- Relative volume at which the material is fully compacted VF=0.10;
- Material viscosity coefficient MU=0.05;
- Bulk viscosity flag (bulk viscosity is not used) BULK=0;
- Elastic modules in uncompressed configuration EAAU=EBBU=ECCU=0.075;
- Shear modules in uncompressed configuration GABU=GBCU=GCAU=0.030;
- Material axes option (globally orthotropic) AOPT=2;
- Material axes change flag (no change) MACF=1;
- Tensile strain at element failure (element will erode) TSEF=0.050;

SOUDASEAL 2K glue
LS-Dyna material type: MAT_27
(MAT_MOONEY-RIVLIN_RUBBER)

This is a two-parametric material model for rubber. The axial force vs. actual change in the gauge length, ΔL, in the uniaxial tension test, required by FE code LS-Dyna, is presented in Fig. 8. Material data, based on Material Card and on the experiments performed by Authors, are collected below:

- Mass density RO=1.45e-6;
- Poisson's ratio PR=0.495;
- Specimen gauge length SGL=30;
- Specimen width SW=5.75;
- Specimen thickness ST=2.3;

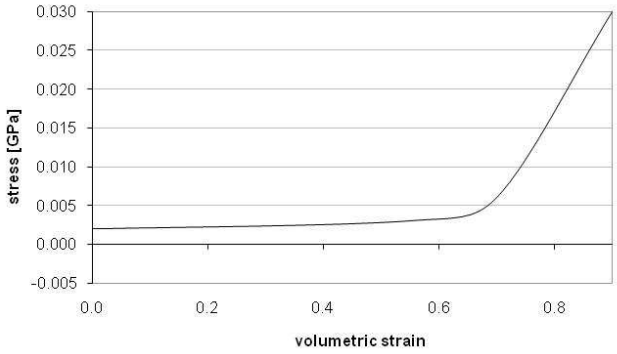

Fig. 7. The normal stress vs. volumetric strain load curve in the uniaxial compression test for ALPORAS aluminium foam

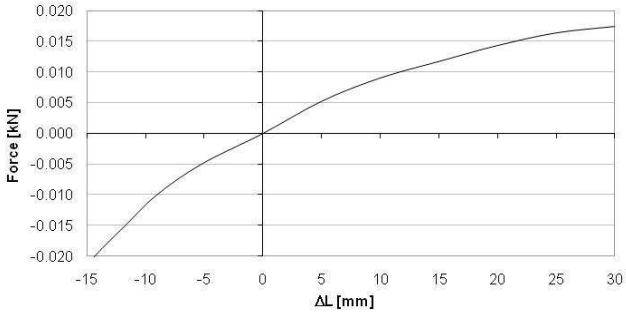

Rys. 8. The axial force vs. the actual change in the gauge length (average experimental data) in the uniaxial tension test for SOUDASEAL 2K glue specimens

The following assumptions are adopted in numerical modelling of the PS and SPS systems loaded by 6 kg TNT blast shock wave (Hallquist, 2009):

- The range stand, erection bolts, the plate stiffening the subsoil and the subsoil work in the linear viscoelastic range. The material models of these components take into account possibility of falling into the plasticity zone. Thus, the assumption related to working range is simply verified during the simulations.
- The external aluminium plate and the protected plate (Armox 500T) work in the elastic–plastic range taking into account high strain rates (the Johnson–Cook model). The plates may be due to large displacements and large plastic deformations.
- Material models corresponding to uniform laminates (S, C, A), ALPORAS aluminium foam, SOUDASEAL 2K glue do not take into account high strain rates, but take into consideration basic failure mechanisms for these materials. The materials undertaken may be due to both large displacements and large deformations.
- Contact and dry friction between respective parts of the PS/SPS systems are taken into account.
- Damping in the protected plate is taken into account according to the constant decrement damping model in the frequency range valuable in the dynamic response of the plate.
- The blast shock wave induced by detonation of HE charge at the central point over the range stand is modelled approximately using the CONWEP model. This model approximates fluid–solid interaction based on the experimental data.
- The initial displacement, strain and stress states induced by the dead load in the PS/SPS systems are neglected.
- The welded joints of erection bolt heads to the protected plate

are reflected approximately by respective constraints.

Blast shock wave was modelled using the LOAD_ BLAST_ENHANCED option offered by LS-Dyna system. This load model defines an airblast function for the application of pressure loads due to explosion of conventional charge, including enhancements for treating reflected waves, moving warheads and multiple blast sources. A type of blast source is spherical free-air burst (BLAST=2).

The exact simulation of the blast/structure interaction using LS-Dyna v971 code requires the use of the burn model described by the velocity of the detonation wave and the thermodynamical parameters on the detonation wave front. This advanced approach is not considered in this study.

The Automatic_Single_Surface steel – steel contact model has been assumed with the static and kinematic friction coefficients equal to 0.10 and 0.05, respectively. In order to minimize penetrations, the Segment_Based_ Contact (SOFT 2) has been selected. The steel – subsoil contact is taken into account with the kinematic friction coefficient equal to 0.20. Moreover, the steel–composite, steel–aluminium foam kinematic friction coefficients are equal to 0.20.

For the protected plate DAMPING_FREQUENCY_ RANGE option has been selected. This option provides approximately constant damping, i.e. frequency independent, over a chosen range of frequencies. The damping parameters amount to (Klasztorny, 2010b): CDAM=0.004 (damping in fraction of critical), FLOW=0.03 (lowest frequency [cycles per ms]), FHIGH=3 (highest frequency [cycles per ms]).

The remaining options in the LS-Dyna solver, selected for blast simulations in the PS and SPS systems, are as follows:

- HOURGLASS control for composites: IHQ-4 CONTACT_ERODING_SINGLE_SURFACE; this is contact taking into account the changes in contacting surfaces resulting from elements erosion;
- FS 2 (DEFINE_FRICTION option);
- VDC 25 (damping in contact);
- SOFT 2 (segment based contact);
- SBOPT 5 (warped segment checking and improved sliding behaviour);
- DEPTH (edge to edge contact);
- CONTROL_TIMESTEP;
- TSSFAC 0.6 (decreasing the time step to 0.6dt);
- ERODE 1 (erosion of the elements for which dt drops below 1% of the initial value; erosion of finite elements with negative volume).

4. RANGE TESTS OF SPS SYSTEM UNDER 6 KG TNT BLAST SHOCK WAVE

The main purposes of experimental – numerical tests performed on energy-absorbing panels ALF joined to the protected plate (Armox 500T) are experimental validation of numerical modelling of the SPS system and assessment of ALF shield effectiveness at 6 kg TNT blast shock wave loading.

The conditions for the experimental test are collected below:

- a spherical charge made of SEMTEX HE material equivalent 6 kg of TNT in reference to the pressure criterion;
- a detonator placed centrally in the sphere;
- central free suspension of HE charge at 400 mm distance from the top surface of the range stand (a typical distance of the vehicle bottom plate from AT mine hidden under the ground surface);
- the range stand resting on the 20 mm thick plate stiffening the subsoil;
- the 450×450×300 mm cubicoidal central hole done under the plate stiffening the subsoil.

Fig. 9. Segment SP with M16 erection bolts before 6 kg g TNT blast test

Fig. 10. The SPS system before 6 kg TNT blast test

Fig. 11. The SPS system after 6 kg TNT blast test

The range experiments were conducted in 2010 on the Navy Academy Range near Strzepcz, Poland. The photo documentation of the experimental blast test is presented in Figs. 9 – 11. Fig. 9 shows the SP segment before 6 kg TNT range test. Figs 10, 11

illustrate the SPS system before and after detonation of 6 kg TNT spherical charge hanged centrally over the stand at the 400 mm vertical distance. High resistance of the stand body is proved experimentally. The erection bolts gave in small plastic deformations. The following damages have been observed:

- valuable plastic deformations and central cracks in the aluminium sheet;
- cracks and delamination of layers in the hybrid laminates,
- failure of glue layers i large areas;
- slight asymmetry of the blast;
- medium plastic deformations and no damages in the protected plate,;
- full compaction and multi-plane breaking of the aluminium foam core.

The deformation contours in reference to the bottom surface of the protected plate in the SPS system after the 6 kg TNT blast, measured using Handyscan scanner are presented in Fig. 12. The plate deformations were quasi-bisymmetric.

5. SIMULATIONS OF DYNAMIC PROCESSES IN THE PS AND SPS SYSTEMS

The simulations correspond to detonation of 6 kg TNT spherical charges in the PS and SPS systems. The results presenting the ALF panel failure picture and plastic deflection of the protected plate in the SPS system have been used to validate experimentally numerical modelling and simulation of the SPS system.

a)

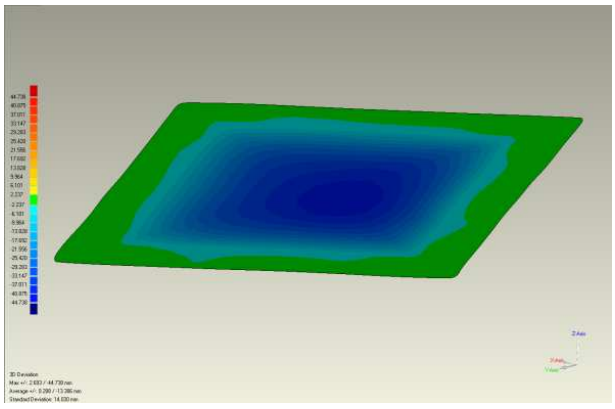

b)

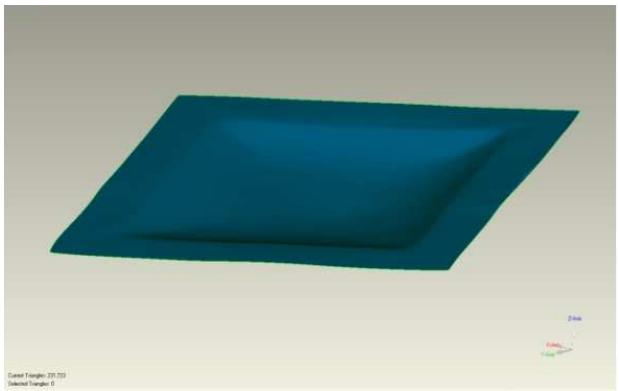

Fig. 12. The plastic deformation 3D scan (performed using Handyscan) for the protected plate removed from SPS system after 6 kg TNT blast: a) the vertical displacement contours; b) the virtual model of the deformed plate

The computations were performed in Department of Mechanics and Applied Computer Science, Military University of Technology, Warsaw, Poland, using LS-Dyna v971 software. The CPU time amounted to ~8 h for the PS system (the real process duration time equals 50 ms), and ~44 h for the SPS system (the real process duration time equals 35 ms). The computations were performed using 8P).

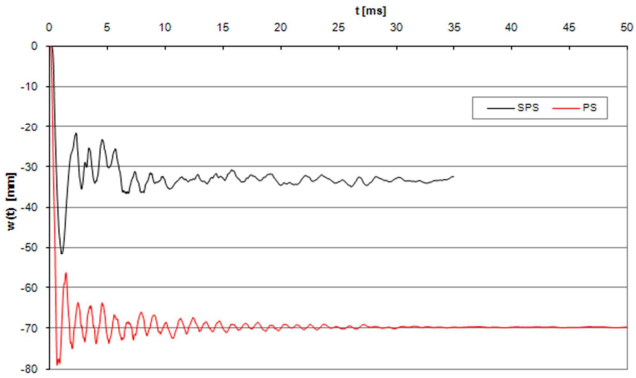

Fig. 13. The SPS and PS systems loaded by 6 kg TNT blast shock wave. Time histories of the relative vertical deflection at the central point of the protected plate

a)

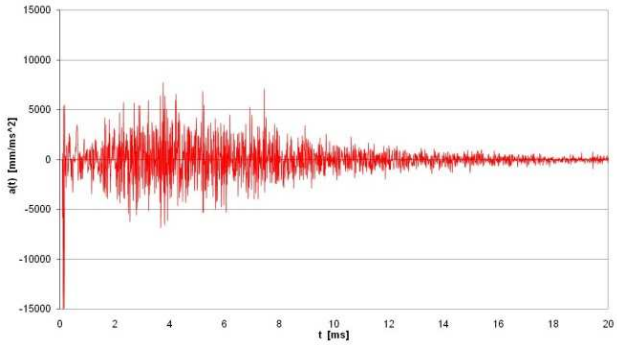

b)

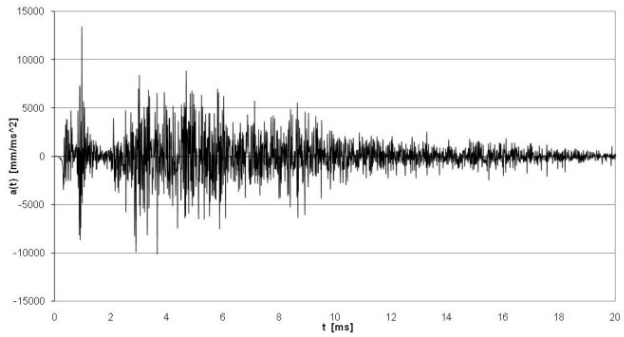

Fig. 14. The PS (a) and SPS (b) systems loaded by 6 kg TNT blast shock wave. Time-histories in the vertical acceeration at the central point of the protected plate

The simulation results are presented in Figs. 12–23. Fig. 13 presents time histories of the relative vertical deflection at the central point of the protected plate in reference to the SPS and PS systems under 6 kg TNT blast. This quantity is understood as the vertical displacement at the midpoint less the vertical displacement at the reference point located in the main cross-section A-A (Fig. 3) at 235 mm distance from the midpoint (at the internal edge

of the central frame). The red line curve, corresponding to the PS system, tends to 70 mm plastic deflection, while the black line curve, related to the SPS system, tends to 33.4 mm plastic deflection. Comparing these deflections enables assessing the effectiveness of the protective panel ALF.

Fig. 14 presents time-histories of the vertical acceleration at the midpoint of the protected plate for the PS system (red line) and the SPS system (black line). The physical correctness of these curves is observed. Small reduction in accelerations at the midpoint of the protected plate is observed. It results from the structural and boundary conditions in both systems. The maximum vertical accelerations overpass time and again the admissible values for a human. Note that the range stand does not reflect LV or LAV vehicle. There are modelled PS and SPS systems and the results cannot be directly interpreted for screw-occupants. One may compare only the maximum values in the PS and SPS systems before developing the algorithm transforming the range results to real vehicles.

Fig. 15 presents the plastically deformed protected plate in the PS system. The next Fig. 16 shows a half of the SPS system in the axonometric view at instant t=1.05 ms corresponding to the maximum vertical deflection in the protected plate. In Fig. 17 one can observe the deformed and partly damaged SP subsystem extracted from the SPS system at the instant corresponding to the maximum vertical deflection in the protected plate.

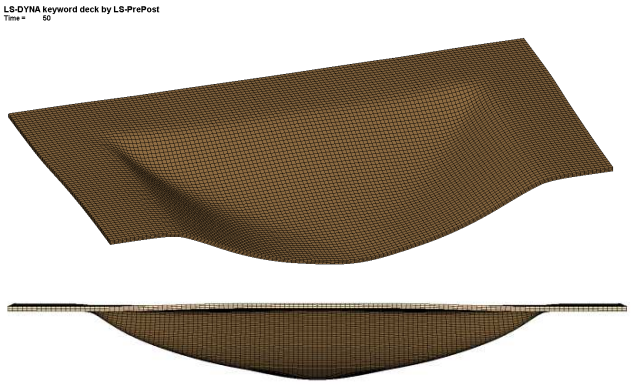

Fig. 15. The deformed protected plate extracted from the PS system after 6 kg TNT blast shock wave. The axonometric view and the side view on the half plate

Fig. 16. The deformed protected plate – ALF panel subsystem extracted from the SPS system loaded by 6 kg TNT blast shock wave. The axonometric view on the half subsystem at t=1.05 sec corresponding to the maximum deflection of the plate

The displacement contours [mm] for the protected plate are presented in Figs. 18 and 19, respectively in the PS and SPS systems under the blast considered. The contours correspond to the instant at which the maximum vertical deflection in the protected plate has occurred. The Huber-Mises-Hencky effective stress contours [GPa] in the protected plate, at the same dynamic conditions, are shown in Figs. 20 and 21. Contours illustrating the effective plastic strains [–] in the protected plate after finishing the dynamic process are presented in Figs. 22, 23 for the PS and SPS systems, respectively.

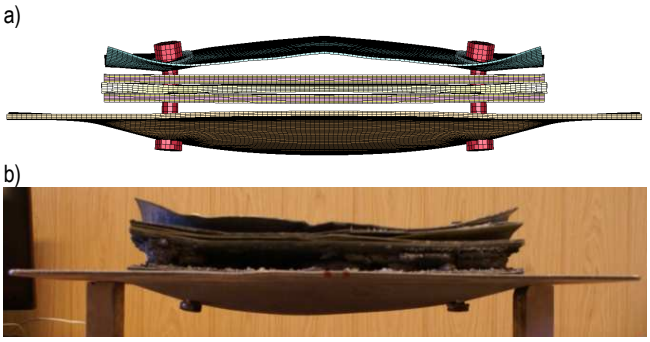

Fig. 17. The SPS system after 6 kg TNT blast shock wave. The side view: a) simulation; b) experiment

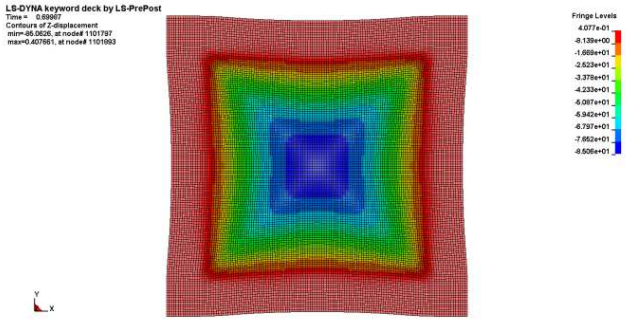

Fig. 18. The PS system loaded by 6 kg TNT blast shock wave. Contours of the vertical displacements [mm] of the protected plate at instant t=0.70 ms (the maximum deflection of the plate)

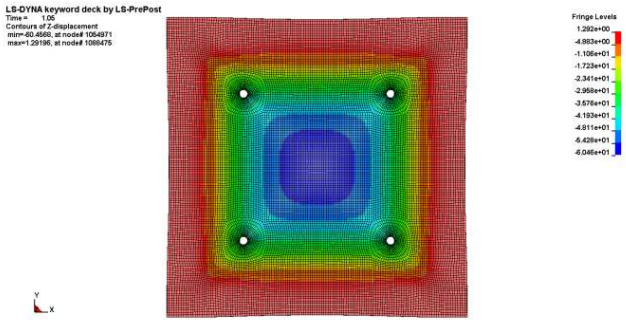

Fig. 19. The SPS system loaded by 6 kg TNT blast shock wave. Contours of the vertical displacements [mm] of the protected plate at instant t=1.05 ms (the maximum deflection of the plate)

The results presented in Figs. 12–23 prove correctness of the physical and numerical modelling as well as simulations of dynamic processes in the PS and SPS systems.

In addition, the internal energy absorbed in the PS and SPS systems, simulated in LS-Dyna, was observed. In the PS system, the absorption amounted to 23.5 kJ; the major part has been absorbed by Armox plate (16.6 kJ), the subsoil absorbed 2.2 kJ, and 4.7 kJ was absorbed by the remaining components, friction

and viscous damping. The SPS system dissipated 53.7 kJ since the vertical distance of the HE charge from the top of the system has been decreased by the ALF panel. The components of the system absorbed the following energies: 34.2 kJ – Alporas foam, 5.3 kJ – Armox plate, 3.9 kJ – Soudaseal glue, 3.4 kJ – hybrid laminates, 3.0 kJ – subsoil, 3.9 kJ – the remaining components, friction and viscous damping.

Impact in the form of the 6 kg TNT blast shock wave induces plastic deformations in the Armox plate in both PS and SPS systems. The plastic deflection can be treated as the measure of these deformations. Respective numerical and experimental values of the plastic deflection are collected in Tab. 6.

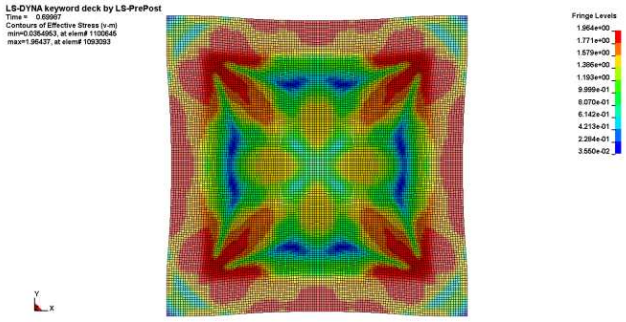

Fig. 20. The PS system loaded by 6 kg TNT blast shock wave. Contours of the Huber-Mises-Hecky effective stresses [GPa] in the protected plate at instant t=0.70 ms (the maximum deflection of the plate)

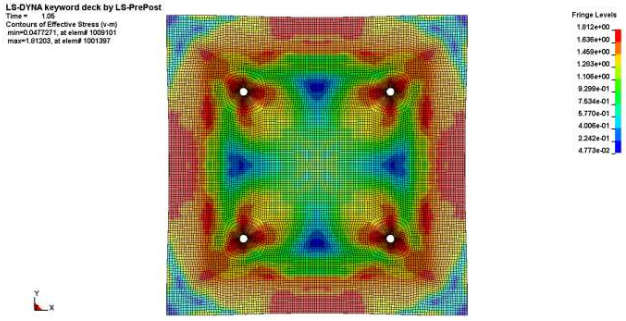

Fig. 21. The SPS system loaded by 6 kg TNT blast shock wave. Contours of the Huber-Mises-Hecky effective stresses [GPa] in the protected plate at instant t=1.05 ms (the maximum deflection of the plate)

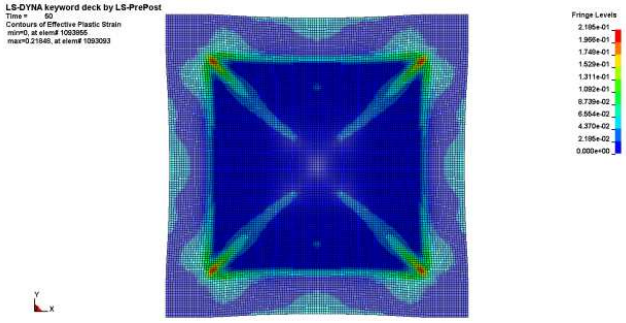

Fig. 22. The PS system after 6 kg TNT blast shock wave. Contours of the effective plastic strains [–] in the protected plate

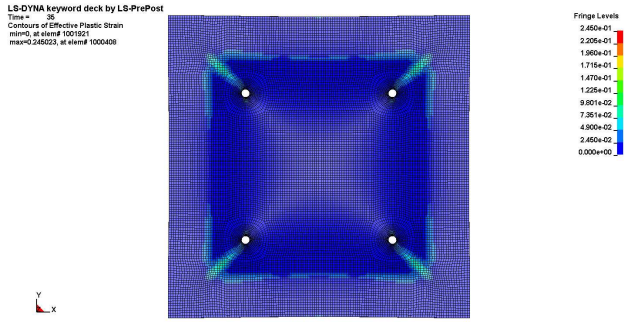

Fig. 23. The SPS system after 6 kg TNT blast shock wave. Contours of the effective plastic strains [–] in the protected plate

Experimental validation of the numerical modelling of the SPS system is measured by the deviation of the numerical plastic deflection from the experimental one. The respective error is defined by the formula:

$$\delta = \frac{|d_N - d_E|}{L} \tag{2}$$

where: d_N – numerical plastic deflection, d_E – experimental plastic deflection, L=470 mm – reference length equal to width of the square hole in the range stand.

Tab. 6. The plastic deflection of the protected plate d [mm] in the PS, SPS systems after 6 kg TNT blast shock wave (N – simulation, E – experiment)

System	6 kg TNT		δ [%]
	N	E	
PS	70.0	–	–
SPS	33.4	38.6	1.1

In reference to the SPS system error is relatively small. Quantitative conformity of the numerical and experimental failure in the ALF shield is assessed positively. Summing up, experimental validation of numerical modelling has been assessed positively with possibility of further improvement of the numerical models. Attention should be put on better modelling of laminate delamination as well as on better modelling of fully compacted aluminium foam at tension. Moreover, the material models describing aluminium foam, hybrid laminates, and glue could be extended on high strain rates.

The effectiveness of the ALF protective shield can be measured by the plastic deflection reduction coefficient defined by the formula

$$\beta = \frac{d_{SPS}}{d_{PS}} \tag{3}$$

where: d_{PS} – plastic deflection in the PS system, d_{SPS} – plastic deflection in the SPS system.

This coefficient is equal to 0.48 for the systems undertaken. Plastic deflection reduction is relatively high and is mainly influenced by the designed stacking structure of the ALF shield as well as by the bolt connections applied in the SPS system.

Within the limits of the Johnson–Cook model the effective stresses in the protected plate reach values 1.96 and 1.81 GPa in the PS and SPS system, respectively. One can observe valuable differences between effective stress contours (in the protected plate) in the PS and SPS systems.

6. CONLUSIONS

Experimental validation of numerical modelling is related to the SPS system loaded by 6 kg TNT blast shock wave. The PS system being the SPS' subsystem does not require separate validation. In the validation, the results of the range test performed in 2010 have been applied. The numerical modelling have been performed for the SPS system (the validation purpose) and for the PS system (the effectiveness assessment purpose). The plastic deflection reduction factor has been calculated.

Based on the numerical – experimental research developed in the study the following final conclusions have been formulated:

- The ALF panels exhibit high relative energy absorption and have the key parameters competitive in the market, i.e. thickness, mass per unit area, protection level, price.
- Experimental validation of numerical modelling of the PS and SPS systems under blast shock waves is positive.
- The design assumptions made for the range stand have been confirmed both experimentally and numerically.

The results corresponding to the selected protective panel and selected HE charge are useful for validation and verification of the numerical model of the protective shield – protected plate – range stand system (SPS). After positive validation and verification one can realize numerical research for other blast conditions or optimize protective panels. Compared to the experiments the simulations are much cheaper and can predict displacement/velocity/acceleration time-histories, effective stress and plastic strain contours for an arbitrary variants of the SPS/PS systems. Such approach enables fast and cheap design of protective panels for required protection level.

REFERENCES

1. **AEP-55,** *Procedures for Evaluating the Protection Levels of Logistic and Light Armoured Vehicles for KE and Artillery Threats*, NATO/PFP Unclassified, Vol. 1.
2. **AEP-55,** *Procedures for Evaluating the Protection Levels of Logistic and Light Armoured Vehicle Occupants for Grenade and Blast Mine Threats Level*, NATO/PFP Unclassified, Vol. 2.
3. **Bachmann H**. (1995), *Vibration problems in structures. Practical guidelines*, Basel – Boston – Berlin, Birkh User.
4. **Hallquist J.O.** (2009), *LS-DYNA. Keyword User's Manual V971 R4 Beta*, LSTC Co., CA, USA.
5. **Jones R.M**. (1975), *Mechanics of composite materials*, McGraw-Hill BC, New York.
6. **Klasztorny M. *et al.*** (2010a), *Application of composite – foam layers for protection from mins and IED. Vol. 1: Composite – foam shields. Final Report. R&D Project No. O R00 0062 06*, Military Univ. Technol, Warsaw, Poland [in Polish].
7. **Klasztorny M. *et al.*** (2010b), Modelling and numerical simulation of the protective shield – protected plate – test stand system under blast shock wave, *Journal of KONES Powertrain & Transport*, Vol. 17, No. 3, 197 – 204.
8. **Klasztorny M. *et al.*** (2010c), Experimental investigations of the protective shield – protected plate – test stand system under blast shock wave, *Journal of KONES Powertrain & Transport*, Vol. 17, No. 4, 229 – 236.
9. **Nillson, M.** (2003), *Constitutive model for Armox 500T and Armox 600T at low and medium strain rates*, Technical Report F01-R-1068-SE, Swedish Defence Research Agency.
10. **STANAG 4190,** *Test Procedures for Measuring Behind-Armour Effects of Anti-Armour Ammunition*, NATO/PFP Unclassified.
11. **STANAG 4569,** *Protection Levels for Occupants of Logistic and Light Armoured Vehicles*, NATO/PFP Unclassified.
12. **Zduniak B., Morka A., Gieleta R.** (2010), Study of FEM model for tension and compression test for aluminium alloys samples in order to set material data, *J. KONES Powertrain & Transport*, Vol. 17, No. 3.